Discharging an Insulator Surface by Secondary Emission Without Redistribution

by

A. S. Jensen

DISCHARGING AN INSULATOR SURFACE BY SECONDARY EMISSION WITHOUT REDISTRIBUTION*

By

ARTHUR S. JENSEN

Research Laboratory, RCA Laboratories,
Princeton, N. J.

Summary—The equations for the complete characteristic curves and discharge factor curves for the developmental Radechon storage tube are derived assuming a Maxwellian energy distribution of secondary electrons, a rectangular uniform beam cross section, and simple target geometry. Comparison of these theoretical curves with measured values is made for several representative tubes with reasonable determination of secondary emission parameters.

Output signal amplitude and signal-to-disturbance ratio equations are derived from aperture theory and the limitations of electron beam cross section, screen mesh and tube output capacitance, again with good agreement with experimental data. These limitations are discussed in a manner that indicates quantitatively the considerations of interest in connection with the design of circuits and systems utilizing the Radechon.

INTRODUCTION

SEVERAL storage tubes[1-3] depend in their operation upon the discharging of an insulator surface by secondary emission in the absence of redistribution. A knowledge of the manner in which this discharge occurs enables one to understand better the operation of such tubes. In particular, the operating characteristic curves of the Radechon can be computed and are in reasonable agreement with experimentally determined curves. Several authors[4-6] already have reported on certain aspects of this problem. Its complexity pre-

---

* Decimal Classification: R138.31.

[1] A. S. Jensen, J. P. Smith, M. H. Mesner, and L. E. Flory, "Barrier Grid Storage Tube and Its Operation," *RCA Review*, Vol. IX, pp. 112-135, March, 1948.

[2] A. S. Jensen, "The Radechon, a Barrier Grid Storage Tube," *RCA Review*, Vol. XVI, pp. 197-215, June, 1955.

[3] R. B. DeLano, Jr., "Large Capacity Storage Tube for Digital-Computer Application," *Proc. I.R.E.*, Vol. 42, p. 626, March, 1954.

[4] J. V. Harrington, "Storage of Small Signals on a Dielectric Surface," *Jour. Appl. Phys.*, Vol. 21, pp. 1048-1053, October, 1950.

[5] C. V. Parker, "Charge Storage in Cathode-Ray Tubes," *Proc. I.R.E.*, Vol. 39, pp. 900-907, August, 1951.

[6] W. W. Weinstock, "An Analysis of Storage Tube Target Action," Master's thesis submitted to the Moore School of Electrical Engineering, University of Pennsylvania, June, 1953.

cludes a complete solution in closed form, and this attempt at solution will make simplifying assumptions also.

The barrier grid target structure of the Radechon consists of a thin sheet of insulator with a fine mesh screen in contact with one side and a metallized plate on the other side. The primary electron beam is incident upon this screen and the surface of the insulator, which surface is usually referred to as the *target* (Figure 1). The screen is relatively thick, the width of an opening being less than twice the thickness of the screen.

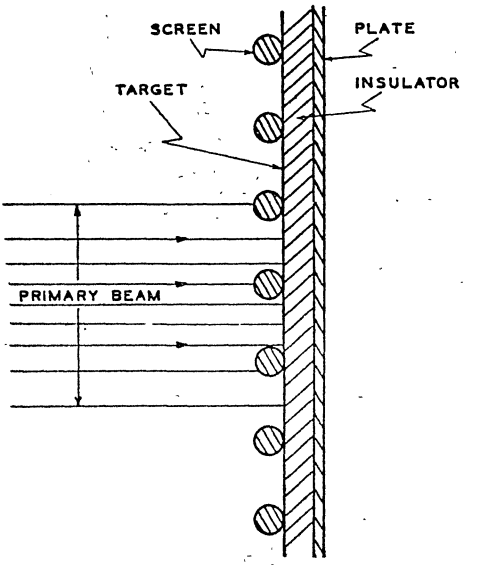

Fig. 1—Target structure.

A schematic diagram of the developmental tube and simplified associated circuits appears in Figure 4 of Reference (2). When the primary beam is incident upon the target surface, secondary electrons are emitted, some of which escape through the screen to the wall as a collector, while the others return to the target. The secondary electron current that escapes to the wall depends upon the relative potential of the target with respect to the screen, upon the energy distribution of the secondaries and upon the secondary emission ratio. The beam current, I_b, flows in the circuit loop as indicated, from the gun via the target to the wall and return. In addition, whenever the capacitance of the target to other electrodes (the sum of all the C_s and C_p in parallel) is being discharged, a discharging current, I_s, flows in the circuit loop as indicated from the target to the wall through the load impedance, R_L and C_L, to return to the screen and plate. Variations of this dis-

charging current through the load impedance constitute the output signal during reading in the Radechon.

Basis of Analysis

To simplify the problem sufficiently to enable its solution in analytical form, the following assumptions have been made:

1. The effect of the screen on the electron optics in front of the target can be approximated by an equipotential plane closely spaced to the target and parallel to it, thus reducing the problem to that of plane, parallel plate geometry.

2. The particular distribution of current in the primary beam is unimportant so that a negligible error results from assuming a rectangular cross section within which the current density is constant.[4]

3. The energy distribution of the secondary electrons is a Maxwellian distribution.[7]

4. Redistribution of secondary electrons is sufficiently restricted by the presence of the screen that those secondaries that return to the insulator return to practically the same point from which they originated.

5. Redistribution within a screen mesh, high velocity primary electrons reflected from edges of screen wires, etc., serve to discharge areas of the target insulator otherwise hidden by the screen from the beam so that the entire target area is involved in the storage process. The screen used in the experimental tubes is a woven mesh with round wires. This assumption was found to be necessary in order to make reasonable values of target capacitance per unit area agree with the experimental data. The final computation of dielectric constant supports this view.

6. The percentage of the primary beam that reaches the insulator and the percentage of the secondaries that reach the wall are constants.

7. Variation in screen transmission ratio, efficiency of collection of secondaries, variations in secondary emission ratio of either insulator or screen, and other uneveness or nonuniformity, all of which generally contribute to the shading and other disturbance signals, are ignored.

8. The secondary emission ratio of the insulator is constant and greater than unity.

9. The switching transient that occurs when the plate voltage is switched from write to read condition or vice versa is ignored, and

[7] K. G. McKay, "A Pulse Method of Determining the Energy Distribution of Secondary Electrons from Insulators," *Jour. Appl. Phys.*, Vol. 22, pp. 89-94, January, 1951.

it is assumed that at all other times the difference in potential between screen and plate is constant.

10. The beam is scanning the target with a constant scan speed.

11. During reading, the beam current is constant.[8]

12. Space-charge effects are ignored; in particular, since the primary beam current density is only about 750 microamperes per square millimeter and the effective screen spacing is about 0.02 millimeter, no space-charge-induced potential minimum is expected between target and screen.[9]

ANALYSIS

Discharging Current Density

For a Maxwellian energy distribution, the current density of secondary electrons leaving the target surface with z-directed energies between eE_z and $e(E_z + dE_z)$ can be expressed in the general form as:

$$\frac{d\rho}{dE_z} = A \exp(-aE_z) \quad \text{for } 0 \leq E_z. \tag{1}$$

The constants of this expression are evaluated such that the total secondary electron current density from the target is $\delta r \rho_b$, and the average secondary electron energy is eE_T. The transmission ratio, r, of the screen enters into this expression since not all of the primary beam reaches the target, some being intercepted by the screen.

$$\frac{d\rho}{dE_z} = \frac{\delta r \rho_b}{E_T} \exp\left(-\frac{E_z}{E_T}\right) \quad \text{for } 0 \leq E_z. \tag{2}$$

This expression is plotted in Figure 2. The total integral under this curve from zero to infinity is just equal to the total secondary electron current density. Of those that leave the target, only those with sufficient energy to reach the screen and penetrate it can escape to the wall (there always being a collecting field between the screen and the wall). This is the integral under the curve between the target potential and infinity, namely:

---

[8] As a result of this assumption, this paper omits the transient response that occurs when the beam current is changed. This transient response is represented by the last term of Equation (12) in Reference (5).

[9] G. C. Sponsler, "Potential Distribution and Prevention of a Space-Charge-Induced Minimum Between a Plane Secondary Electron Emitter and Parallel Control Grid," *Jour. Appl. Phys.*, Vol. 25, pp. 282-287, March, 1954.

$$\rho_w = \int_{E_z}^{\infty} \frac{d\rho}{dE_z} dE_z. \tag{3}$$

This gives

$$\rho_w = \delta r \rho_b \exp\left(-\frac{E_z}{E_T}\right) \quad \text{for } 0 \leq E_z \tag{4a}$$

$$\rho_w = \delta r \rho_b \quad \text{for } E_z \leq 0. \tag{4b}$$

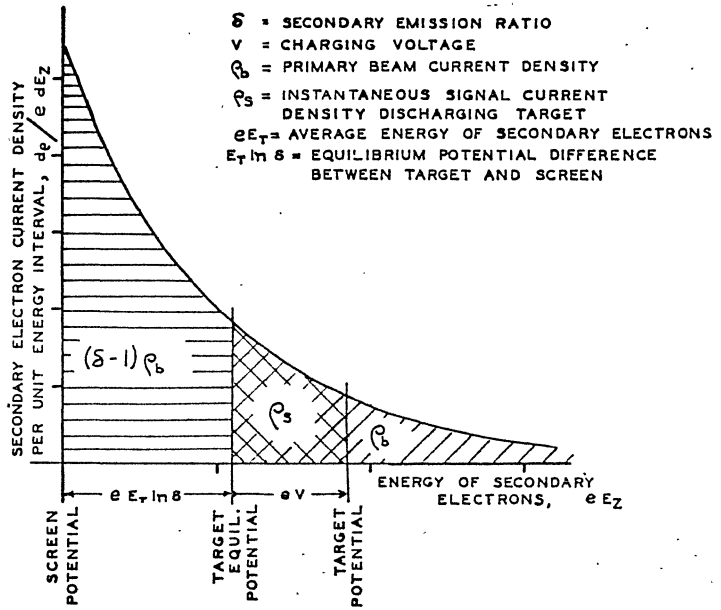

Fig. 2—Energy distribution of secondary electrons.

The remaining secondary electrons, those that do not escape through the screen, fall back again to the target, being restricted by the screen to return to virtually the same points from which they originated. It is evident from the circuit of Figure 4 of Reference (2) that the difference between the primary current density that reaches the target and the current density escaping to the wall is available to discharge the target capacitance.

$$\rho_s = r\rho_b - \rho_w. \tag{5}$$

Again, the screen transmission ratio enters the calculation since only that fraction of the beam can contribute towards discharging the

target. There is a target potential for which there is no further discharging, for which the current density escaping to the wall is just equal to the primary current density. This is known as the *equilibrium potential.* From Equation (4) this is seen to be

$$E_z = E_T \ln \delta \qquad \text{for } \rho_s = 0 \text{ and } \rho_w = r\rho_b. \tag{6}$$

It is important to note that the electron beam can only discharge the target toward this equilibrium potential. Changes in potential of the target away from equilibrium can only be made by applying a signal to the plate. This equilibrium potential makes a convenient choice for an axis, with respect to which target potentials are expressed as

$$V = E_z - E_T \ln \delta. \tag{7}$$

With this choice of axis, the discharging current density becomes

$$\rho_s = r\rho_b \left[1 - \exp\left(-\frac{V}{E_T} \right) \right] \qquad \text{for } -E_T \ln \delta \leq V \tag{8a}$$

$$\rho_s = r\rho_b (1-\delta) \qquad \text{for } V \leq -E_T \ln \delta. \tag{8b}$$

Final Potential after Discharge

A particular elemental target area can be discharged only while under bombardment by the primary beam. The total effect of this

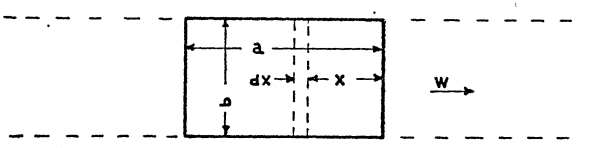

Fig. 3—Assumed scanning beam cross section.

discharging can be evaluated by integrating the changes in potential as the beam scans over the element, as in Figure 3. The potential of the target elements as a function of their position, x, with respect to the scanning beam can be computed by solving the equation

$$\int_V^{V_x} dV = -\int_0^{x/W} \frac{\rho_s}{C_x} dt \tag{9}$$

while the beam is scanning at speed W. (Here x is measured from the front edge of the sharply defined assumed beam shown in Figure 3.

Later, in connection with Figure 10 of Reference (2), the same letter is used as a measure from the center of a real spot.)

There are three different cases, each resulting in a different solution for Equation (9). In Case I, when the target potential is always positive with respect to the screen, Equation (8a) may be substituted in Equation (9), and the integration made directly. Similarly, in Case III, when the target potential is always negative with respect to the screen, Equation (8b) is substituted before integration. However, in Case II, when the target potential is initially negative to that of the screen but ultimately is positive, the problem must be broken into two parts, using Equations (8b) and (8a) respectively. The solutions are

Case I $[-E_T \ln \delta \leq V]$

$$V_x = V + E_T \ln\left\{\left[1 - \exp\left(-\frac{V}{E_T}\right)\right] \exp\left(-\frac{r\rho_b x}{C_x W E_T}\right) + \exp\left(-\frac{V}{E_T}\right)\right\} \tag{10a}$$

Case II $[J_b E_T(1-\delta) - E_T \ln \delta \leq V \leq -E_T \ln \delta \leq V_x]$

$$V_x = V + E_T \ln\left[\exp\left(-\frac{V}{E_T}\right) + (1-\delta) \exp\left\{-\frac{r\rho_b x}{C_x W E_T} + \frac{\delta}{1-\delta}\left(\frac{V}{E_T} + \ln \delta\right)\right\}\right] \tag{10b}$$

Case III $[V \leq J_b E_T(1-\delta) - E_T \ln \delta]$

$$V_x = V - \frac{r\rho_b(1-\delta)x}{C_x W}. \tag{10c}$$

The relative beam current

$$J_b \equiv \frac{r\rho_b a}{C_x W E_T} \equiv \frac{\gamma a}{W} \equiv \frac{r I_b}{C_x b W E_T}. \tag{11}$$

One can write the expressions for the final target potential after the complete passage of the beam in the form[10]

[10] Equations (12a) and (15a) of this paper are identical respectively to Equations (5) and (10) of Reference (5).

Case I $[-E_T \ln \delta \leq V]$

$$V_b = V + E_T \ln \left\{ \left[1 - \exp\left(-\frac{V}{E_T}\right) \right] \exp\left(-J_b\right) + \exp\left(-\frac{V}{E_T}\right) \right\} \tag{12a}$$

Case II $[J_b E_T(1-\delta) - E_T \ln \delta \leq V \leq -E_T \ln \delta \leq V_b]$

$$V_b = V + E_T \ln \left[\exp\left(-\frac{V}{E_T}\right) + (1-\delta) \exp\left\{ -J_b + \frac{\delta}{1-\delta}\left(\frac{V}{E_T} + \ln \delta\right) \right\} \right] \tag{12b}$$

Case III $[V \leq J_b E_T(1-\delta) - E_T \ln \delta]$

$$V_b = V - J_b(1-\delta)E_T. \tag{12c}$$

Signal Current

The signal current observed at the output of the tube is the sum of all the discharging currents from the target elements under bombardment. Referring to Figure 3,

$$I_s = \int_0^a b\rho_s dx, \tag{13}$$

the integration being over the entire spot area in accordance with assumption (5). Again, there are three cases for solution, and substituting Equations (8) and (10), writing for the relative signal current,

$$J_s = \frac{I_s}{C_x b W E_T} \tag{14}$$

which is similar to Equation (11), one obtains[10]

Case I $[-E_T \ln \delta \leq V]$

$$J_s = -\ln \left\{ \left[1 - \exp\left(-\frac{V}{E_T}\right) \right] \exp\left(-J_b\right) + \exp\left(-\frac{V}{E_T}\right) \right\} \tag{15a}$$

Case II $[J_b E_T(1-\delta) - E_T \ln \delta \leq V \leq -E_T \ln \delta]$

$$J_s = -\ln \left[\exp\left(-\frac{V}{E_T}\right) + (1-\delta) \exp\left\{ -J_b + \frac{\delta}{1-\delta}\left(\frac{V}{E_T} + \ln \delta\right) \right\} \right] \tag{15b}$$

Case III $[V \leq J_b E_T(1-\delta) - E_T \ln \delta]$

$$J_s = (1-\delta)\, J_b. \tag{15c}$$

Characteristic Curves

Since this signal current constitutes the output signal for the tube, curves plotted from these equations are the characteristic curves for the tube's operation.[11] Families of such curves are plotted in Figures 4 and 5 and also in Figure 6 of Reference (2) for three different Radechons; measured values are plotted for comparison.[12] The three regions of the curves corresponding to the three cases of solution are marked on the graph. Note in particular that for higher J_b the point

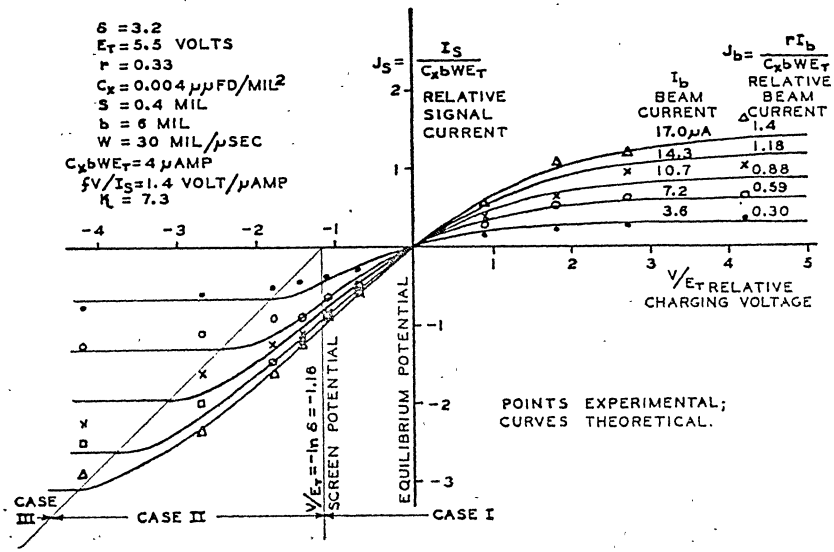

Fig. 4—Target characteristics of an experimental Radechon.

on the negative portion of the curve where the tangent becomes horizontal moves out to the left according to

$$V/E_T = (1-\delta)J_b - \ln \delta \tag{16}$$

and the region over which the curve is tolerably straight increases, particularly in the negative direction.

Note also, that for a given value of relative charging voltage,

[11] In plotting these curves, V is taken as the charging voltage applied to the plate with respect to the screen, ignoring the capacitive divider effect of C_s and C_p, since this effect is not significantly large.

[12] Operating data for the developmental tubes was obtained by M. D. Harsh and W. H. Sandford, Jr. of the Tube Division, Lancaster, Pa.

V/E_T, the output signal is a decreasing function of J_b, becoming more linear with respect to J_b as V increases. Such current characteristic curves are essentially cross sections of the above figures and are plotted, together with measured values for comparison, in Figures 6 and 7. This indicates that for simple signal storage operation in which a signal is written at one time and read out later, it is desirable to write with variable beam current (signal applied to the control grid) while a charging voltage of approximately 20 volts is applied on the plate with respect to the screen, and to read with a large steady beam current after the plate has been returned to the same potential as the screen.

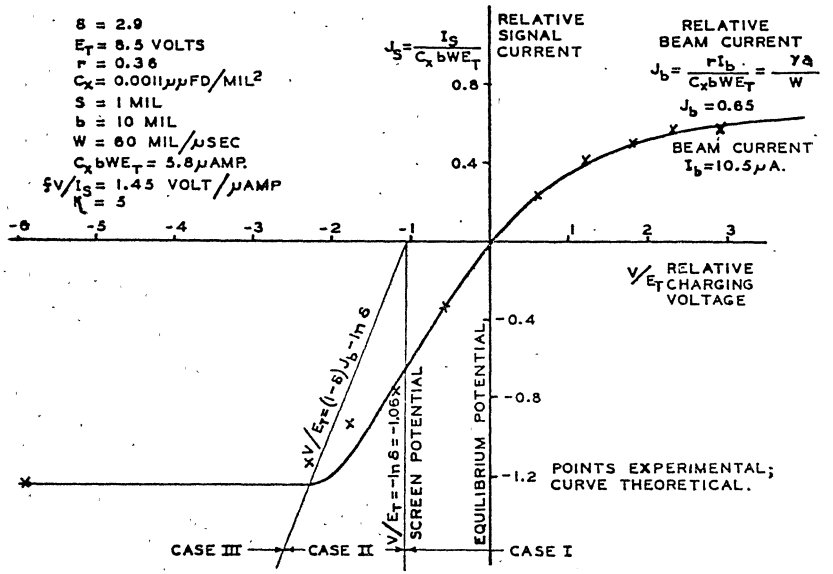

Fig. 5—Target characteristics of an STE-S type experimental Radechon.

The charging voltage of the target during reading is determined by the charge deposited during writing.

The theoretical curves plotted in the preceding figures were fitted to the measured values by an appropriate choice of four parameters: secondary emission ratio of the insulator (δ), average energy of secondary electrons (eE_T), screen transmission ratio (r), and target capacitance per unit area (C_x). The reasonableness of the fit lends credence to the values chosen for these parameters so that this plotting of the curves becomes a means for their measurement. It is of special interest that the secondary emission ratio of mica at 1200 volts, with contamination normally expected from standard tube construction, is close to 3.0, and that the average energy of secondary electrons from

the mica is about 8 electron-volts, which is somewhat higher than that for metals and possibly somewhat higher than its true value, since the target does not actually have the plane, parallel plate geometry assumed in the derivation.

It is possible to compute the dielectric constant of the mica target from the value of target capacitance per unit area that had to be assumed and the known target thickness. For the three tubes, this was 5, 7, and 5 respectively, encouragingly close to the published value for mica (5.66 to 5.97, Elsas, 1891).

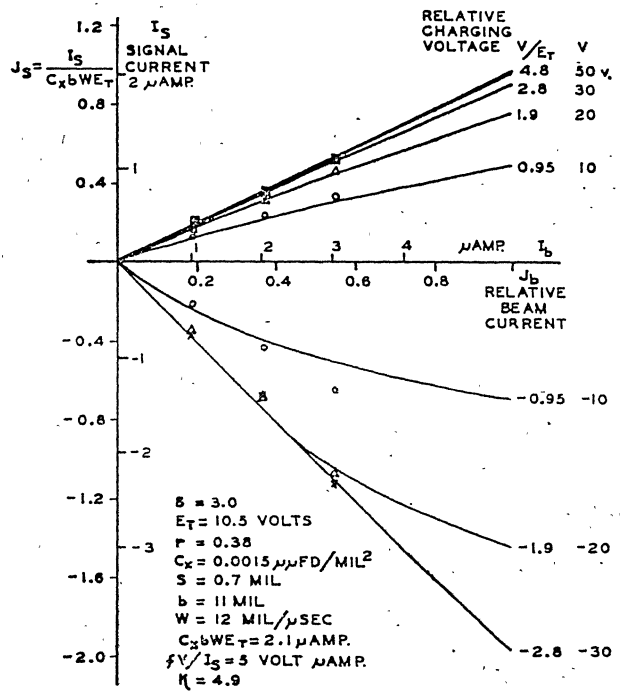

Fig. 6—Current characteristics of the developmental type Radechon.

Discharge Factor

It is evident from Equations (12) that, since the beam is incident upon any small area of the target for only a limited time, this target area cannot be completely discharged. To facilitate the discussion of such discharging, an important concept has been evolved. The *discharge factor, f,* is defined as the ratio between the voltage difference through which the target capacitance has been discharged by one passage of the beam and the target's initial voltage difference from equilibrium.

$$f \equiv \frac{V - V_b}{V}. \tag{17}$$

From this definition and Equations (12) and (15), it follows that for all three cases

$$f = \frac{E_T J_s}{V}. \tag{18}$$

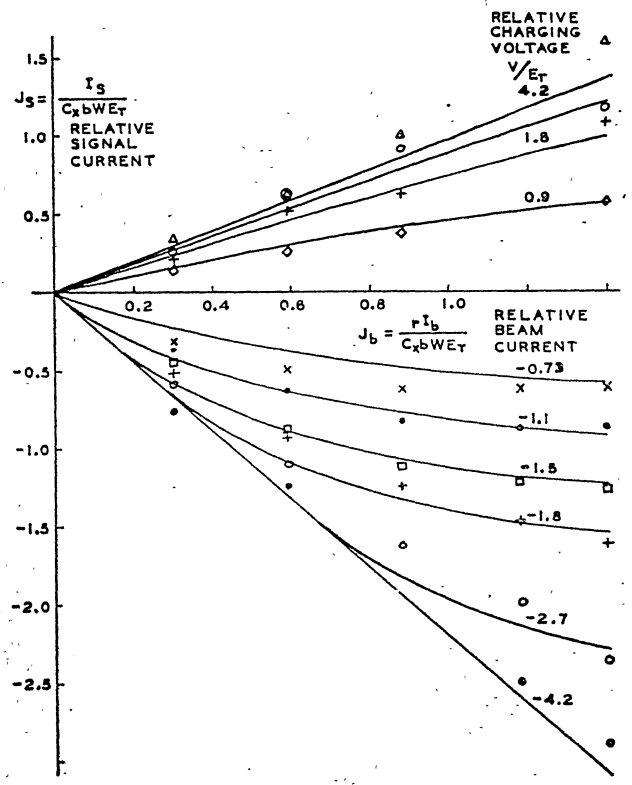

Fig. 7—Current characteristics of an experimental Radechon.

Thus the discharge factor is the slope of the chord of the target characteristic (Figures 4 and 5) drawn from the origin to the curve at the relative charging voltage applied. Therefore, a curve of discharge factors can be computed graphically for a tube once a target characteristic is available. Figure 5 is the target characteristic of an early experimental tube for which many measurements of discharge factor were made. These experimental values, slopes of the chords to the experimental points on the target characteristic, and values com-

puted from Equation (18) are all plotted in Figure 8 for comparison. Their mutual agreement indicates the firmness of the theory.

The discharge factor depends on the relative beam current in much the same way as does the relative signal current. A family of discharge factor curves for the developmental tube is plotted in Figure 8 of Reference (2).

Output Signal Amplitude

Resolution: Output Current For Varying Signal

The output signal current, I_s, discussed so far and plotted in the graphs is that for a quasi-static or slowly varying signal. In any real case, the signals vary in amplitude rapidly and the charge pattern

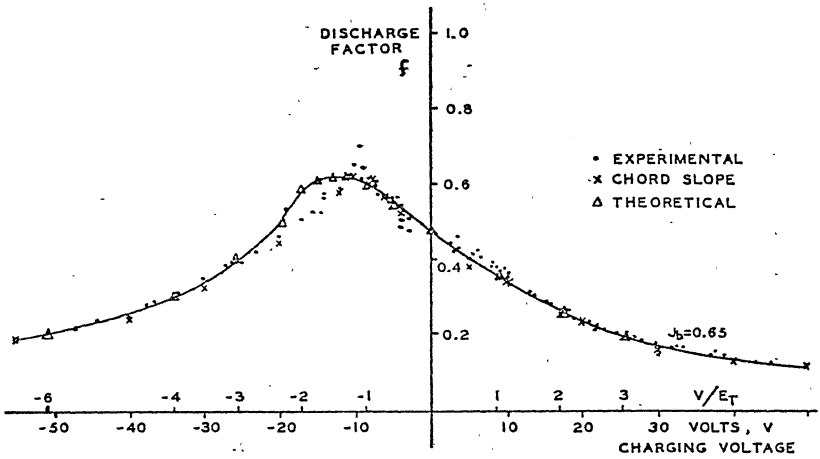

Fig. 8—Discharge factor for the STE-S type experimental Radechon.

stored on the dielectric target has dimensions not greater than a few beam spot widths. In this case errors in writing and reading this charge pattern are introduced by the finite size of the spot, which acts as a scanning aperture.[13] Any particular signal must both be written and read so that the storage tube actually comprises two such apertures in cascade. Therefore, the effective aperture is $b\sqrt{2}$ where b is the spot size (Equation (29) of Reference (13)). This results in a decrease in output signal current amplitude with increased number of signal cycles per target diameter in a manner described in Figures 14 and 15 of Reference (13). These curves are analogous to the transient response of low-pass electrical networks with sharp cutoff.

[13] O. H. Schade, "Electro-Optical Characteristics of Television Systems, Part II," *RCA Review*, Vol. IX, pp. 245-286, June, 1948.

Aperture correction networks,[14] comprising, for example, two cascaded R-C stages in the output amplifier, can compensate for this low-pass effect in much the same manner that high-peaking circuits are used in standard television camera practice to compensate for a large R-C constant at the image-orthicon output, at the expense of both high-frequency noise and disturbance.

This correction to account for the signal variations must be applied to I_s in all the equations in this paper.

Resolution: Spot Size Measurement

In every discussion of resolution, it must be remembered that real electron beam spots do not have sharp boundaries; therefore, any specification of spot size should include the method of measurement. In the method employed here, a sharp-edged metal ribbon 40 mils wide was placed on the target structure. The strip was then scanned and the output signal observed on an oscilloscope using a wide-band amplifier (Figure 10, Reference (2)). The length of the transient response of this unit step function was measured from the 10 to the 90 per cent amplitude response points and compared with the total width of the signal from the ribbon. This is roughly equivalent to measuring the spot width at the 44 per cent current density level, or at $x = 0.9$ for a beam whose current density varies as $\exp(-x^2)$. This differs somewhat from the definition used in Reference (13) which took $x = 2$. Making this correction and introducing the factor for cascading two apertures, one obtains the effective aperture given in the resolution curves[12] of Figure 9 of Reference (2), which in turn agree, both in the value of resolution at which the curve begins to fall off and in the slope of that fall off, with Figure 15 of Reference (13). (Schade's value of relative line number (N/N_δ) is approximately our $(4nb\sqrt{2}/x)$ and is equal to unity at 70 lines per target diameter for the developmental Radechon.)

This method of scanning the edge of a metal ribbon measures the current distribution across the spot. Actually, the pertinent quantity is the charge deposited on the target. But, since the charging of a capacitance is nonlinear, those portions of the beam that discharge the target most completely, operate at the least efficiency. This means that as the discharge factor is increased, the center of the beam becomes less efficient in discharging; the edges become more important and the spot effectively flattens out and becomes larger. Thus, as the

[14] Further references and better circuits can be found in R. C. Dennison, "Aperture Compensation for Television Cameras," *RCA Review*, Vol. XIV, pp. 569-585, December, 1953.

discharge factor is increased, particularly above 0.5, the resolution is decreased.

Signal Output

The storage tube is essentially a high-internal-impedance current generator, so that the simplified equivalent output circuit is that of Figure 9, in which the signal current, I_s, is determined by the tube characteristics as described above and V_s is the voltage signal appearing on the grid of the first amplifier tube.

$$V_s = \frac{I_s}{C_L\sqrt{\omega_L^2 + \omega^2}} \tag{19}$$

where

$$\frac{\omega_L}{2\pi} = \frac{1}{2\pi R_L C_L} \tag{20}$$

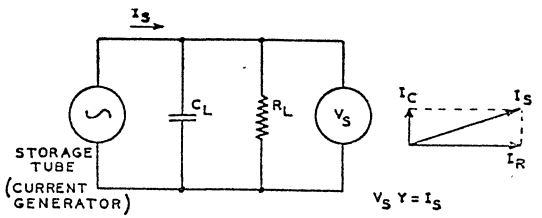

Fig. 9—Equivalent output circuit.

is the output bandwidth and $\omega/2\pi$ is the reading signal frequency. For a well-designed system, $\omega = \omega_L$ for the highest expected signal frequency. Taking n as the number of stored signal cycles per unit length of scan,

$$\omega_L = 2\pi W_r n \tag{21}$$

and

$$V_{sr} = \frac{I_{sr}}{2\pi W_r n C_L\sqrt{2}} \tag{22}$$

as the value of the stored signal input to the amplifier, where the subscripts r indicate that this is during reading.

Disturbance Signal

For the beam currents and current densities used to obtain a high discharge factor, the most serious disturbance is that generated by

scanning across the screen wires. This signal can be shown to be about 7 times as large as the thermal noise at the input of the preamplifier and about 100 times the shot noise. The maximum amplitude of the disturbance signal, I_d, is determined by that fraction of the beam which is intercepted by one screen wire so that

$$I_d = \frac{(\sigma - 1) u I_{br}}{a} \tag{23}$$

where σ is the secondary emission ratio of the screen wires (measured to be between 0.98 and 1.1), and u is the wire diameter. With $N = 1/\lambda$, where N is the screen mesh per unit length and λ the distance from center to center of the wires, the maximum screen disturbance frequency is

$$\omega_d = 2\pi N W_r, \tag{24}$$

and the disturbance signal becomes, from Equation (19),

$$V_{dl} = \frac{(\sigma - 1) u I_{br}}{2\pi a W_r C_L \sqrt{n^2 + N^2}}, \tag{25}$$

the subscript r denoting reading. Typical values are $u = 1$ mil, $\sigma = 1.1$, and $N = 230$ per inch. The signal-to-disturbance ratio is then,

$$D \equiv \frac{V_{sr}}{V_d} = \frac{I_{sr}}{I_{br}} \frac{a}{(\sigma - 1) u} \frac{\left[1 + \left(\frac{N}{n}\right)^2\right]^{1/2}}{\sqrt{2}}. \tag{26}$$

This ratio is the number of gray levels reproducible as halftones in a signal. In agreement with Equation (26), this ratio has been about 30 for a resolution of about 300 lines per target diameter and a relative writing-beam current of 0.37. Note that this relation indicates that signal-to-disturbance ratio is a negative function of the system design resolution.

Simple Storage Operation

For simple signal storage in which a signal is written and then read out later, writing should be done with $V/E_T \simeq 2.5$ for which, from Equations (12), the change in voltage accomplished by depositing charges on the target is

$$\Delta V = V_b - V = -E_T J_{bw}, \tag{27}$$

the subscript w denoting the writing operation. Reading is accomplished at a fixed beam current for which $J_{br} \simeq 0.5$. The reading discharge factor is practically constant for all values of signal used; in this region $f_r \simeq J_{br} \leq 0.50$. From Equations (18) and (27) we obtain: $J_{sr} = -f_r J_{bw}$ and, dropping the minus sign, $J_{sr} = J_{bw} J_{br}$, or $I_{sr} = r J_{bw} I_{br}$,

$$V_{sr} = \left(\frac{r^2}{2\pi C_x b E_T C_L \sqrt{2}} \right) \frac{I_{bw} I_{br}}{W_w W_r n} \tag{28}$$

this being the value of the first reading signal output following a single writing. The linearity of this signal with writing- and reading-beam currents is noteworthy, since it indicates that the Radechon can reproduce halftone signal values.

Both the signal-to-disturbance ratio (D) and the signal-to-noise ratio (S/N) are limitations to the use of the tube. In particular, when the tube is operated as recommended in the preceding paragraph

$$\frac{D W_w n}{I_{bw}} = \left(\frac{r^2 N}{C_x E_T (\sigma - 1) \pi \sqrt{2}} \right). \tag{29}$$

This indicates that the maximum writing speed is inversely proportional to both the signal-to-disturbance ratio and the resolution required.

Likewise the signal-to-noise ratio, while usually considerably greater than the signal-to-disturbance ratio, may limit the reading conditions since,

$$(S/N) \equiv \frac{V_{sr}}{V_n} = \left(\frac{r^2}{4 C_x b E_T \sqrt{\pi C_L k T}} \right) \frac{I_{bw} I_{br}}{W_w W_r n}. \tag{30}$$

where V_n is the thermal noise in the output resistor. When chosen for the desired bandwidth,

$$V_n = \left(\frac{2kT}{\pi C_L} \right)^{1/2}. \tag{31}$$

Conclusions

When many simplifying assumptions must be made to enable the analytical solution of a problem, and when some of the parameters

such as the secondary emission ratio, the average energy of the secondary electrons, and even the target thickness are not well known and may vary from tube to tube, one cannot depend entirely upon theoretical calculations. However, the number of instances in which measured results have agreed with the foregoing theory have been sufficient to be very encouraging. In this respect these equations have value in indicating the manner in which the Radechon should be used in storage applications and the limitations to be expected in its operation.